

Possible Phases of the Strong Interaction Vacuum¹

Shuqian Ying
Physics Department, Fudan University
Shanghai 200433, China
and
CCAST (World Laboratory), P. O. Box 8730
Beijing 100080, China

September 26, 2018

¹Talk given at the *Multiplicity Production and Heavy Ion Collision* Workshop held at CCAST (World Laboratory), Beijing, Mar. 4-9, 1996

Abstract

A study of the possible vacuum phases in a strongly interacting two flavor light quark system is presented. Four possible phases are found with some of their properties presented. The possible existence of a localized diquark condensed phases inside a nucleon and excited hadrons is investigated by showing the potential of solving three selected current “puzzles” in experimental observations if such a possibility is taken into account. Base on these results, the potential of producing these phases in heavy ion collisions is speculated.

Contents

1	A General Introduction	3
I	Theoretical Exploration	5
2	Preliminaries	6
2.1	Introduction	6
2.2	Auxiliary field method using a simple model as an example	7
2.3	8-component Dirac spinor	8
3	Models	10
3.1	Classification of the 4-fermion interaction terms	10
3.2	Model 1 and its vacuum phase diagram	11
3.3	Model 2 and its vacuum phase diagram	13
3.4	Spontaneous separation of baryon number in the β - and ω - phases	15
II	Traces of β- and ω- Phases in Nuclear Systems	17
4	Extended PCAC Relation for a Nucleon	19
4.1	A QCD chiral Ward identity and PCAC relation	19
4.2	PCAC relation for nucleon states	20
4.3	Chiral symmetry and two basics relations between nucleon form factors	20
4.4	The determination of valid q^2 region	21

4.5	Test of PCAC relation for a nucleon	22
4.6	Extended PCAC relation for a nucleon	25
5	Gerasimov–Drell–Hearn Sum Rule for a Nucleon	27
5.1	Photon–nucleon compton scattering	27
5.2	Sum rules and infinite momentum frame	28
5.3	Regge behaviors and physical states	29
5.4	Gauge invariance constraints	29
5.5	The possibility of modifying GDH sum rule	30
6	Rapidity Correlation of $B\bar{B}$ in High Energy e^+e^- Annihilation	31
7	Summary and Outlook	33

Chapter 1

A General Introduction

The strong interaction vacuum is believed to undergo certain kind of phase transition in high temperature and density environments. Such a belief at high temperature is substantiated by both lattice QCD computations [1] and the statistical bootstrap argument [2] of the early days when the fundamental particles of strong interaction are considered to be baryons, mesons and corresponding resonances. The destination phases of the transition from the present day large scale strong interaction vacuum phase, in which the temperature and density can be regarded as zero, and the nature of these transitions remain, however, poorly understood. The best known new phase of QCD is the one called quark–gluon plasma (QGP), which was found on lattice QCD simulations [1]. Other phases, such as the chiral symmetry restoration phase [3], was also shown to happen together with the QGP in lattice QCD calculations.

To understand these questions is a worthwhile endeavor since, on the one hand, the behaviors of QCD are not known well enough to have all its possible phases listed with their properties predicted and, on the other hand, the experimental probes of the hadronic matter in the laboratories and the analysis of resulting data have not provided us with sufficiently clear pictures for the nature of the vacuum phases produced. For example, it is still not known for certain whether or not the QGP has been created in heavy ion collisions. However, an understanding of the above mentioned problems is of fundamental importance since the knowledge gained in this area can help us to understand the evolution of the early universe, the properties of the stellar matters in heavy stars, and eventually to tell, e.g., where matter come from, why there appears to be an arrow for the time, etc.. It thus constitutes one of the frontiers of our knowledge that awaits to be explored.

QCD is a highly nonlinear theory that is difficult to solve, especially at low and intermediate energies. Lattice simulations are still limited by the power of computers, which allows the computation only on small lattice (size) systems. In addition, fermions are not easy to handle on lattices. The approach adopted by this study for the theoretical explorations is to use simplified fermionic models for the strong interaction which inherit most of the basic symmetries of QCD at long distances. These models can be considered to have large overlap with the ones that are derivable by integrating the gluon degrees of freedom (in the path integration sense) out from the original QCD Lagrangian density. Despite such an expectation may in fact not easily fulfilled in reality, we still consider this undertaken valuable since it can provide sharp predictions that can be compared to our empirical knowledge due to the relative simplicity of the model approaches. In addition, the simplicity of the model approach can let us investigate large set of possibilities (for the fermionic sector) that is otherwise not possible. In contrast to the theoretical exploration efforts, the model dependency of the study related to realistic physical systems, in which the theoretical possibilities is searched for, is reduced as much as possible by using model independent methods like, e.g., symmetry constraints, sum rules, etc.. In doing so, the conclusion

derived can be more reliable.

On the observational sides, the information about a nucleon in various reactions, the multiplicity production in e^+e^- annihilation and many others can be used to determine whether the theoretical possibilities discovered in model studies actually exist inside static systems like a nucleon and in a time dependent system like in the e^+e^- annihilation system. Albeit a negative result of the above mentioned investigations does not necessary mean that these possibilities are forbidden in other processes like heavy ion collisions, which are the main topic of this workshop, the early universe, etc., a positive result from these “domestic” experiments does increase the probabilities and are thus worth of studying. In addition, the structure of a nucleon, the hadronization mechanism in the e^+e^- annihilation are interesting problems on their own rights.

The report consists of two parts. In the first part, which is based on Refs. [4, 5] and work undertaken Ref. [6], two massless fermionic models for the strong interaction are introduced with their vacuum phase structure determined. The massless fermions are identified as up (u) and down (d) quarks. Four kinds of phases are found: 1) the bare vacuum 2) the so called α -phase, in which the original chiral $SU(2)_L \times SU(2)_R$ symmetry is spontaneously broken down to a flavor $SU(2)_V$ symmetry, that is widely studied in literature 3) the β -phase, in which the original chiral $SU(2)_L \times SU(2)_R$ symmetry is also spontaneously broken down to a flavor $SU(2)_V$ symmetry; it spontaneously breaks the $U(1)$ symmetry corresponding to baryon number conservation induced by a condensation of diquarks 4) the ω -phase, in which the original chiral $SU(2)_L \times SU(2)_R$ symmetry is unbroken. The $U(1)$ symmetry corresponding to baryon number conservation is also spontaneously broken, like in the β -phase. The second part consists of a study of three different issues. The first one is related to an examination of the PCAC relationship for a nucleon, which is based upon Ref. [7]. Certain inconsistency that is in favor of the existence of a localized β -phase inside a nucleon is revealed. The second one provides a gauge invariant modification of the Gerasimov-Drell-Hearn (GDH) sum rule required by current experimental data. It is based upon Ref. [8]. If the deviation of the experimental data from the GDH sum rule is proven genuine, a spontaneous broken down of the $U(1)$ symmetry correspond to baryon number conservation inside a nucleon is shown to be a necessity. One of the most natural realization of such a symmetry breaking is by having β - or ω - phase inside a nucleon. The third one is based upon the observed baryon-antibaryon rapidity difference correlation in a high energy e^+e^- annihilation which is discussed by Prof. Xie’s group [9] in Shandong University in this workshop. Experimental evidence exists [10] that baryon number and antibaryon number is not locally produced in the observed jets. Such a violation of locality can be shown to be a direct consequence of the fact that the string that fragments in to hadrons contains either the β - or ω - phase. In the last chapter of this report, a summary is provided and some speculations concerning the possibility of producing the β - or/and ω - phases is given.

Part I

Theoretical Exploration

Chapter 2

Preliminaries

2.1 Introduction

The basic participants of the strong interaction we know of today are color carrying quarks (antiquarks) and gluons with basic interaction between them mediated by gluons according to the QCD Lagrangian density, which is a non-Abelian gauge theory with asymptotic freedom at short distances or high energies. At low and intermediate energies, the interaction between color sources (including quarks and gluons) becomes strong enough to render a perturbative analysis useless. For a light quark system, strong interaction can cause quark–antiquark pair production from the bare vacuum. With the increase of the interaction strength, it is expected that a macroscopic number of quark–antiquark pairs can be produced resulting in effects that survive the thermal limit to lead to various phase transitions in the vacuum.

At a formal level, the gluon degrees of freedom can be integrated out to obtain a pure quark–quark interaction effective action. Such an effective quark–quark interaction action are expected to be very complicated if can be practically computed at all and difficult to analyze to extracting useful information without certain physical picture being built up using other indirect approaches. One of these approaches is to build models for the quark–quark interaction part that inherits the basic symmetries of the original Lagrangian density. It is expected that the major physics emerged from these models has large overlap with the one implied by the QCD Lagrangian.

Before list the symmetries considered, let's make the first simplification. The behaviors of certain massless fermion system are expected to represent the light quark system, which is restricted to the up (u) and down (d) quark sector in the flavor space here, well. Thus, for the simplicity of the discussion, we shall assume that the mass of the u and d quarks is zero. QCD Lagrangian density with massless u and d quarks has, besides the ones listed in the following, a $SU(2)_L \times SU(2)_R$ chiral symmetry. So the symmetries that these models should have in addition are 1) invariance under the Lorentz group 2) global $U(1)$ symmetry corresponding to the conservation of baryon number 3) local $U(1)_{em}$ symmetry corresponding to the electromagnetism 4) global color $SU(3)_c$ symmetry.

One of the well studied model with the above properties is the Nambu Jona–Lasinio (NJL) model [11] used at the light quark level (some include the strange quark as well).

2.2 Auxiliary field method using a simple model as an example

The fermion–fermion interaction terms are assumed to be of contact 4–fermion form in the first part of the report. One of the best methods of treating these nonlinear 4–fermion interaction models is to introduce auxiliary fields [12, 13]. The subtleties of introducing auxiliary fields related to the Fierzing \mathcal{F} and Crossing \mathcal{C} operations are discussed in more detail in Ref. [5]. It shall not be discussed here. Suffice it will be to use the following heuristic steps to show how auxiliary fields are introduced to handle these non-linear terms.

For simplicity, let's consider the following fermion–fermion interaction model

$$\mathcal{L} = \bar{\psi} (i\rlap{\not{\partial}} - m) \psi + G_0 (\bar{\psi}\psi)^2, \quad (2.2.1)$$

where m is the mass of the fermion, ψ is a 4–component Dirac spinor fermion field and G_0 is the coupling constant.

In the path integration formalism, the generating functional $W[\eta, \bar{\eta}]$ for the connected Green functions for the fermions is

$$\exp(iW[\eta, \bar{\eta}]) = N \int D[\psi] D[\bar{\psi}] \exp \left[i \int d^4x (\mathcal{L} + \bar{\eta}\psi + \bar{\psi}\eta) \right], \quad (2.2.2)$$

where $\eta, \bar{\eta}$ are external Grassmanian fields, N is a constant that are of no physical effects; it is so chosen that $W[0, 0]$ is zero.

Since the fermion fields are not bilinear in the argument of the exponential integrand, the functional integration over the fermion fields can not be easily computed. A step forward can be achieved if the following mathematical transformation is used, namely,

$$\begin{aligned} \exp(iW[\eta, \bar{\eta}]) &= N' \int D[\psi] D[\bar{\psi}] \exp \left[i \int d^4x (\mathcal{L} + \bar{\eta}\psi + \bar{\psi}\eta) \right] \\ &\times \int D[\sigma] \exp \left[-i \int d^4x (a\sigma + b\bar{\psi}\psi)^2 \right], \end{aligned} \quad (2.2.3)$$

where σ is the auxiliary field introduced and a, b are arbitrary constant to be determined in the following. The second functional integration over σ gives an η and $\bar{\eta}$ independent constant contribution since it is a complete square in the argument of the exponential been integrated; it causes no physical consequences since its effects can be absorbed in to the normalization constant N' . After writing the generating functional in this form, progress can be made by a proper choice of the constants a and b . Let $a = 1/2\sqrt{G_0}$ and $b = \sqrt{G_0}$, then Eq. 2.2.3 is

$$\exp(iW[\eta, \bar{\eta}]) = N' \int D[\sigma] \int D[\psi] D[\bar{\psi}] \exp \left[i \int d^4x (\mathcal{L}' + \bar{\eta}\psi + \bar{\psi}\eta) \right] \quad (2.2.4)$$

with

$$\mathcal{L}' = \bar{\psi} (i\rlap{\not{\partial}} - \sigma - m) \psi - \frac{1}{4G_0} \sigma^2. \quad (2.2.5)$$

When the space–time dimension is taken to be $1 + 1$, this is the half bosonized Gross–Neveu model [13]. It can be seen that the 4–fermion term in the original Lagrangian density are absent in the new one; this allows the integration over the fermion fields be carried out. The price that one should pay

is to introduce additional field,, namely the auxiliary field σ , to be functionally integrated. Eq. 2.2.4 becomes

$$\exp(iW[\eta, \bar{\eta}]) = N' \int D[\sigma] \exp(iS_{eff}[\sigma] + \bar{\eta} S_F \eta), \quad (2.2.6)$$

where the effective action S_{eff} for the auxiliary field σ after integrate the fermion fields can be expressed as

$$S_{eff}[\sigma] = -i\text{SpLn}\gamma^0(i\cancel{\partial} - \sigma - m) - \frac{1}{4G_0} \int d^4x \sigma^2, \quad (2.2.7)$$

with “Sp” denoting the functional trace of the corresponding operator. Formally, S_{eff} can be expressed in terms of the eigenvalues λ of operator $\hat{D} \equiv \gamma^0(i\cancel{\partial} - \sigma - m)$, namely,

$$S_{eff}[\sigma] = -i \sum_{\lambda} \ln \frac{\lambda[\sigma]}{\lambda[0]} - \frac{1}{4G_0} \int d^4x \sigma^2, \quad (2.2.8)$$

where $\lambda[\sigma]$ is the eigenvalue of \hat{D} and the summation is over all of the eigenvalues considered.

In case of σ independent of space-time, which is the case for the vacuum state of the system, Eq. 2.2.8 can be simplified further to

$$S_{eff}(\sigma) = -iV_4 \int \frac{d^4p}{(2\pi)^4} \ln \left[\frac{p^2 - (\sigma + m)^2}{p^2 - m^2} \right] - \frac{1}{4G_0} V_4 \sigma^2, \quad (2.2.9)$$

where $V_4 \rightarrow \infty$ is the space-time volume of the system. The vacuum σ value of the system can be determined by minimizing the effective potential $V_{eff}(\sigma) = -S_{eff}(\sigma)/V_4$.

2.3 8-component Dirac spinor

The best representation for the Dirac spinor for the path integral formalism developed in this study is the 8-component “real” one [4, 5, 6] as oppose to the 4-component one. An 8-component “real” Dirac spinor can be written as

$$\Psi = \begin{pmatrix} \psi_1 \\ \psi_2 \end{pmatrix}, \quad (2.3.10)$$

where ψ_1 and ψ_2 are 4-component Dirac spinors. They are related to each other in the following way

$$\psi_2 = \begin{cases} C\bar{\psi}_1^T & \text{One flavor} \\ Ci\tau_2\bar{\psi}_1^T & \text{Two flavor} \end{cases} \quad (2.3.11)$$

where $C = -C^{-1}$ is the charge conjugation operator (in the 4-component representation of the Dirac spinor) and τ_2 is the second Pauli matrices acting on the flavor space of the fermion field Ψ .

For later discussions, it proves useful to introduce three Pauli matrices $O_{1,2,3}$ acting on the two 4-component Dirac spinor $\psi_{1,2}$. With O_i , Eq. 2.3.11 can be more compactly written as

$$\bar{\Psi} = \Psi^T \Omega, \quad (2.3.12)$$

with the Ω matrix defined as

$$\Omega = \begin{pmatrix} 0 & -C^{-1}\rho^{-1} \\ C\rho & 0 \end{pmatrix}, \quad (2.3.13)$$

where $\rho = \rho^{-1} = 1$ for one flavor case and $\rho = i\tau_2 = -\rho^{-1}$ for two flavor case.

Using the 8-component Ψ , the Lagrangian density corresponding to Eq. 2.2.5 takes to following form

$$\mathcal{L}' = \frac{1}{2}\bar{\Psi}(i\not{\partial} - \sigma - m)\Psi - \frac{1}{4G_0}\sigma^2. \quad (2.3.14)$$

The effective action for σ is then

$$S_{eff}[\sigma] = -\frac{i}{2}\text{SpLn}\gamma^0(i\not{\partial} - \sigma - m) - \frac{1}{4G_0}\int d^4x\sigma^2 + const \quad (2.3.15)$$

due to Eq. 2.3.12. Here “*const*” is chosen such that $S_{eff}[0] = 0$.

Chapter 3

Models

3.1 Classification of the 4-fermion interaction terms

The light quark system in reality contains fermionic u and d quarks with three colors. Therefore the fermion fields that should be used (in the 4-component form) is $4 \times 2 \times 3 = 24$ component. For a modeling of the quark system, a Dirac spinor ψ_{fc} with $f = u, d$ labeling the flavor and $c = 1, 2, 3$ labeling the color has to be used. For the compactness, the flavor and color indices of ψ will be suppressed in the following as long as no confusion is thought to occur.

If the mass of the light quarks is assumed to be zero, the full Lagrangian density of the system is written as

$$\mathcal{L} = \bar{\psi} i \not{\partial} \psi + \mathcal{L}_{int}. \quad (3.1.1)$$

The 4-fermion interaction terms can be generally classified into two categories in the quark-antiquark channel

$$\begin{aligned} \mathcal{L}_{int} &= \left. \begin{array}{c} \bar{q} \searrow \quad \nearrow \bar{q} \\ \bullet \\ q \nearrow \quad \searrow q \end{array} \right\} \text{color singlet} + \left. \begin{array}{c} \bar{q} \searrow \quad \nearrow \bar{q} \\ \bullet \\ q \nearrow \quad \searrow q \end{array} \right\} \text{color octet} + \text{Fierz term} \\ &= \mathcal{L}_{int}^{(0)} + \mathcal{L}_{int}^{(8)}, \end{aligned} \quad (3.1.2)$$

where $\mathcal{L}_{int}^{(0)}$ generates quark-antiquark scattering in color singlet channel and $\mathcal{L}_{int}^{(8)}$ generates quark-antiquark scattering in color octet channel.

For $\mathcal{L}_{int}^{(0)}$, the well known two flavor chiral symmetric Nambu Jona-Lasinio (NJL) [11] interaction is chosen, namely

$$\mathcal{L}_{int}^{(0)} = G_0 \left[(\bar{\psi} \psi)^2 + (\bar{\psi} i \gamma^5 \vec{\tau} \psi)^2 \right]. \quad (3.1.3)$$

The color octet $\mathcal{L}^{(8)}$ is written in the quark-quark (antiquark-antiquark) channel form for our purposes, namely

$$\mathcal{L}_{int}^{(8)} = \left. \begin{array}{c} q \searrow \quad \nearrow \bar{q} \\ \bullet \\ q \nearrow \quad \searrow \bar{q} \end{array} \right\} \text{color triplet} + \left. \begin{array}{c} q \searrow \quad \nearrow \bar{q} \\ \bullet \\ q \nearrow \quad \searrow \bar{q} \end{array} \right\} \text{color sextet} + (q \leftrightarrow \bar{q})$$

$$= \mathcal{L}_{int}^{(3)} + \mathcal{L}_{int}^{(6)}. \quad (3.1.4)$$

The color sextet term is repulsive in the one gluon exchange case. Due to the non-existence of colored baryon containing three quarks in nature, it is assumed to be generally true. So we restrict ourselves to the attractive color triplet two quark interaction terms. The attractive color triplet quark bilinear terms can be classified according to their transformation properties under Lorentz and chiral $SU(2)_L \times SU(2)_R$ groups. In general, if only terms without derivative in fermion fields are considered, $\mathcal{L}_{int}^{(3)}$ has the following form

$$\mathcal{L}_{int}^{(3)} = \frac{1}{2} \sum_r G_r \sum_{ab} C_{ab}^r (\bar{\psi} \Gamma_a^r \tilde{\psi}) (\tilde{\psi} \Gamma_b^r \psi), \quad (3.1.5)$$

with Γ_a^r, Γ_b^r matrices in Dirac, flavor and color spaces generating representation “ r ” and satisfying the antisymmetrization condition

$$\left(\Gamma_{a,b}^r i\tau_2 C \right)^T = -\Gamma_{a,b}^r i\tau_2 C, \quad (3.1.6)$$

for the fermionic systems.

Operator $\tilde{\psi} \Gamma_b^r \psi$ belongs to an irreducible representation “ r ” of chiral, Lorentz and color groups and $\bar{\psi} \Gamma_a^r \tilde{\psi}$ belongs to the conjugate representation. Coefficients C_{ab}^r render the summation $\sum_{ab} \dots$ invariant under Lorentz, chiral $SU(2)_L \times SU(2)_R$ and color $SU(3)_c$ groups. $\{G_r\}$ is a set of independent 4-fermion coupling constants characterizing the color triplet quark-quark interactions. The tilded fermion field operators $\tilde{\psi}$ and $\bar{\tilde{\psi}}$ are defined as

$$\tilde{\psi} = \psi^T (-i\tau_2) C^{-1}, \quad (3.1.7)$$

$$\bar{\tilde{\psi}} = C i\tau_2 \bar{\psi}^T. \quad (3.1.8)$$

The transformation properties of a list of bilinear products of two fermion fields in color triplet and sextet representations are given in Table 1, where all of the possible ones without any derivative in fermion fields are included.

3.2 Model 1 and its vacuum phase diagram

The 4-fermion interaction terms are classified in the above section. The representation “2” of table 3.1 is chosen to form the first model interaction term. In terms of the 8-component Dirac spinor Ψ and after half bosonization [5, 6], it takes the following form

$$\begin{aligned} \mathcal{L}_1 = & \frac{1}{2} \bar{\Psi} \left[i\not{\partial} - \sigma - i\vec{\pi} \cdot \vec{\tau} \gamma^5 O_3 - \gamma^5 \mathcal{A}_c \chi^c O_{(+)} - \gamma^5 \mathcal{A}^c \bar{\chi}_c O_{(-)} \right] \Psi \\ & - \frac{1}{4G_0} (\sigma^2 + \vec{\pi}^2) + \frac{1}{2G_{3'}} \bar{\chi}_c \chi^c, \end{aligned} \quad (3.2.9)$$

where $\sigma, \vec{\pi}, \bar{\chi}_c$ and χ^c are auxiliary fields, $(\chi^c)^\dagger = -\bar{\chi}_c$, G_0 and $G_{3'}$ are coupling constants of the model.

Table 3.1: Transformation properties of various bilinear fermion operators under the action of Lorentz, chiral $SU(2)_L \times SU(2)_R$ and color $SU(3)_c$ groups.

Representation	Operators	Lorentz Group	$SU(2)_L \times SU(2)_R$	$SU(3)_c$
1	$\tilde{\psi}\psi$	<i>Pseudoscalar</i>	1 <i>dim</i>	$\bar{3}$
2	$\tilde{\psi}\gamma^5\psi$	<i>Scalar</i>	1 <i>dim</i>	$\bar{3}$
3	$\begin{pmatrix} \tilde{\psi}\tau\psi \\ \tilde{\psi}\gamma^5\tau\psi \end{pmatrix}$	<i>Pseudoscalar</i> <i>Scalar</i>	6 <i>dim</i>	$\bar{6}$ $\bar{6}$
4	$\begin{pmatrix} \tilde{\psi}\gamma^\mu\psi \\ \tilde{\psi}\gamma^\mu\gamma^5\tau\psi \end{pmatrix}$	<i>Axial Vector</i> <i>Vector</i>	4 <i>dim</i>	$\bar{6}$ $\bar{6}$
5	$\begin{pmatrix} \tilde{\psi}\gamma^\mu\gamma^5\psi \\ \tilde{\psi}\gamma^\mu\tau\psi \end{pmatrix}$	<i>Vector</i> <i>Axial Vector</i>	4 <i>dim</i>	$\bar{3}$ $\bar{3}$
6	$\tilde{\psi}\sigma^{\mu\nu}\psi$	<i>Tensor</i> −	1 <i>dim</i>	$\bar{6}$
7	$\begin{pmatrix} \tilde{\psi}\sigma^{\mu\nu}\tau\psi \\ \tilde{\psi}\sigma^{\mu\nu}\gamma^5\tau\psi \end{pmatrix}$	<i>Tensor</i> − <i>Tensor</i> +	6 <i>dim</i>	$\bar{3}$ $\bar{3}$

If the auxiliary fields do not depend on the space-time, the effective potential can be computed in the momentum space, it has the following form

$$\begin{aligned}
V_{eff} = & 4i \int \frac{d^4p}{(2\pi)^4} \ln \left[\left(1 - \frac{\sigma^2 + \chi^2}{p^2} \right)^2 - \frac{\sigma^2}{p^2} \left(1 - \frac{\sigma^2 - \chi^2}{p^2} \right)^2 \right] \\
& + \frac{1}{4G_0} \sigma^2 + \frac{1}{2G_{3'}} \chi^2,
\end{aligned} \tag{3.2.10}$$

where $\chi^2 \equiv -\bar{\chi}_c \chi^c$.

A numerical evaluation in Euclidean momentum space shows that the minima of $V_{eff}(\sigma, \chi)$ is located on either the σ axis ($\chi = 0$) or the χ axis ($\sigma = 0$). $V_{eff}(\sigma, 0)$ and $V_{eff}(0, \chi)$ are found to be

$$v_{eff}(\sigma, 0) = 3f\left(\frac{\sigma^2}{\Lambda^2}\right) + \frac{1}{16\pi\alpha_0} \frac{\sigma^2}{\Lambda^2}, \tag{3.2.11}$$

$$v_{eff}(0, \chi) = 2f\left(\frac{\chi^2}{\Lambda^2}\right) + \frac{1}{16\pi\alpha_{3'}} \frac{\chi^2}{\Lambda^2}, \tag{3.2.12}$$

where Λ is the Euclidean p^μ space cutoff that defines the model, the dimensionless effective potential is defined by $V_{eff} \equiv \Lambda^4 v_{eff}$, $\alpha_0 = G_0 \Lambda^2 / 4\pi$ and $\alpha_{3'} = G_{3'} \Lambda^2 / 8\pi$ with

$$f(x) = \frac{1}{8\pi^2} \left[-x + \ln \left(1 + \frac{1}{x} \right) x^2 - \ln(1+x) \right]. \tag{3.2.13}$$

The value of V_{eff} at the minima of Eqs. 3.2.11 and 3.2.12 determine the vacuum of the system in the one loop Hartree–Fock approximation for the fermions. It is easy to represent the phase structure of the model by showing it in the α_0 – $\alpha_{3'}$ plane, which is given by Fig. 3.1. Three kinds of phases for

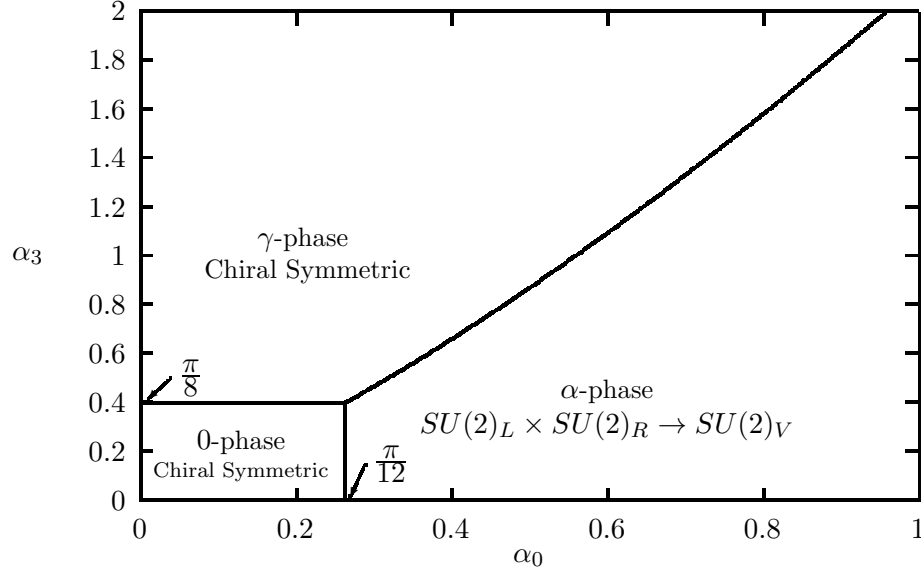


Figure 3.1: The phase boundaries between the α -phase, γ -phase and the 0-phase. The chiral symmetry is unbroken in both the γ -phase and the 0-phase. The α -phase breaks the chiral symmetry spontaneously down to a flavor symmetry.

the vacuum are possible. The first phase, which is called the 0-phase, is the bare vacuum. The second phase, or the α -phase, has non-vanishing average value of $\bar{\Psi}\Psi$; the chiral $SU(2)_L \times SU(2)_R$ symmetry is spontaneously broken down to a $SU(2)_V$ flavor symmetric one in this phase. The third phase, defined as the ω -phase, has non-vanishing diquark and anti-diquark condensation characterized by a non-vanishing χ^2 ; chiral symmetry is unbroken in this phase.

The phase transition across the boundary between the 0- and the α - phases ($\alpha_0^c = \pi/12$) and the one between the 0- and the ω - phases ($\alpha_{3'}^c = \pi/8$) are of second order. The phase transition between the α - and the ω - phases ($\alpha_0 > \pi/12$ and $\alpha_{3'} > \pi/8$) is of first order. The Meissner effects for the electromagnetic field are present in the ω -phase. This is discussed in more detail in Ref. [5] for model II in the following. We shall relegate such a discussion for this model to other work.

3.3 Model 2 and its vacuum phase diagram

The second model interaction Lagrangian density chosen are constructed from the ones in representation “4” of table 3.1. In terms of the 8-component Dirac spinor Ψ and after half bosonization [5, 6], its Lagrangian density is

$$\mathcal{L}_2 = \frac{1}{2} \bar{\Psi} \left[i \not{\partial} - \sigma - i \vec{\pi} \cdot \vec{\tau} \gamma^5 O_3 + O_{(+)} \left(\phi_\mu^c \gamma^\mu \gamma^5 \mathcal{A}_c + \vec{\delta}_\mu^c \cdot \vec{\tau} \gamma^\mu \mathcal{A}_c \right) \right] \Psi$$

$$\begin{aligned}
& -O_{(-)} \left(\bar{\phi}_{\mu c} \gamma^\mu \gamma^5 \mathcal{A}^c + \vec{\bar{\delta}}_{\mu c} \cdot \vec{\tau} \gamma^\mu \mathcal{A}^c \right) \Big] \Psi - \frac{1}{4G_0} (\sigma^2 + \vec{\pi}^2) \\
& - \frac{1}{2G_{3'}} (\bar{\phi}_{\mu c} \phi^{\mu c} + \vec{\bar{\delta}}_{\mu c} \cdot \vec{\delta}^{\mu c}),
\end{aligned} \tag{3.3.14}$$

where $\bar{\phi}_{\mu c}$, ϕ_μ^c with $(\phi_\mu^\dagger)_c = -\bar{\phi}_{\mu c}$, $\vec{\bar{\delta}}_{\mu c}$, $\vec{\delta}_\mu^c$ with $(\vec{\delta}_\mu^\dagger)_c = -\vec{\bar{\delta}}_{\mu c}$ are auxiliary fields introduced.

The effective potential V_{eff} can be computed. A numerical evaluation of it in the Euclidean momentum space shows that the absolute minimum of $V_{eff}(\sigma^2, \phi^2)$ is located either at $\sigma^2 \neq 0$ and $\phi^2 = 0$, which is the α -phase, or at $\sigma^2 = 0$ and $\phi^2 \neq 0$, which is called the β -phase, in the spontaneous symmetry breaking phases. The phase diagram is obtained by minimizing V_{eff} with respect to ϕ^2 by assuming $\sigma^2 = 0$ in the β -phase and with respect to σ^2 by assuming $\phi^2 = 0$ in the α -phase. The result is represented in Fig.3.2. When $\sigma^2 = 0$ or $\phi^2 = 0$ explicit expressions for the effective potential can be

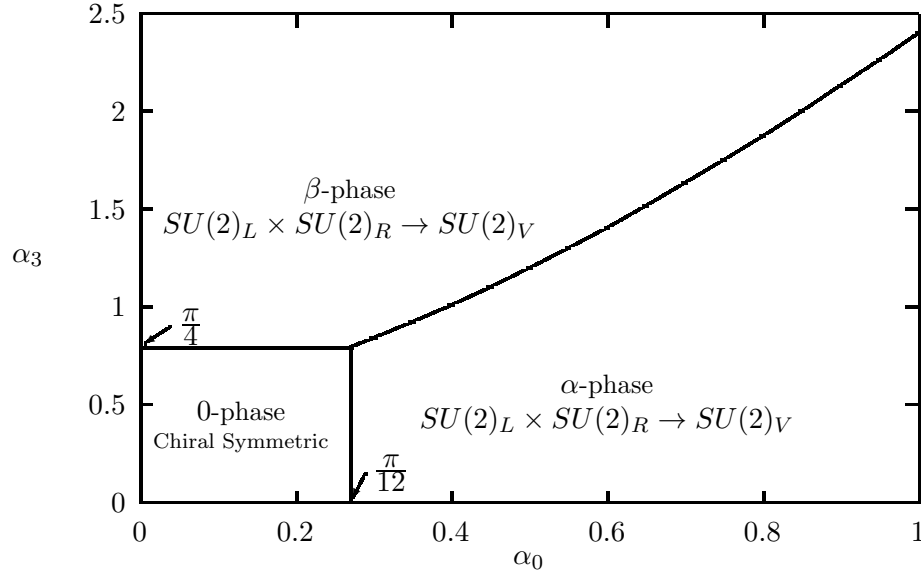


Figure 3.2: The phase boundaries between the α -phase, β -phase and the 0-phase. The chiral symmetry is unbroken in the 0-phase. The α -phase and β -phase break the chiral symmetry spontaneously down to a flavor symmetry.

derived. They are

$$V_{eff}(\sigma^2, 0) = \frac{\Lambda^4}{4\pi} \left\{ \frac{1}{4} \left(\frac{1}{\alpha_0} - \frac{6}{\pi} \right) \frac{\sigma^2}{\Lambda^2} + \frac{3}{2\pi} \ln \left(1 + \frac{\Lambda^2}{\sigma^2} \right) \frac{\sigma^4}{\Lambda^4} - \frac{3}{2\pi} \ln \left(1 + \frac{\sigma^2}{\Lambda^2} \right) \right\}, \tag{3.3.15}$$

and

$$V_{eff}(0, \phi^2) = \frac{\Lambda^4}{4\pi} \begin{cases} \frac{1}{4} \left(\frac{1}{\alpha_3} - \frac{4}{\pi} \right) \frac{\phi^2}{\Lambda^2} + \frac{1}{6\pi} \frac{\phi^4}{\Lambda^4} & \phi^2 \leq \Lambda^2 \\ \frac{1}{4\alpha_3} \frac{\phi^2}{\Lambda^2} - \frac{1}{2\pi} \left(1 + 2 \ln \frac{\phi^2}{\Lambda^2} + \frac{2}{3} \frac{\Lambda^2}{\phi^2} \right) & \phi^2 > \Lambda^2 \end{cases}, \tag{3.3.16}$$

with the reduced dimensionless coupling constants α_0 and α_3 defined as

$$\alpha_0 = \frac{G_0 \Lambda^2}{4\pi}, \quad (3.3.17)$$

$$\alpha_3 = \frac{G_3 \Lambda^2}{8\pi}. \quad (3.3.18)$$

The value of σ^2 that minimize $V_{eff}(\sigma^2, 0)$ satisfies

$$\frac{\sigma^2}{\Lambda^2} \ln \left(1 + \frac{\Lambda^2}{\sigma^2} \right) = \left(1 - \frac{\pi}{12\alpha_0} \right). \quad (3.3.19)$$

It can not be solved explicitly. The value of ϕ^2 that minimize $V_{eff}(0, \phi^2)$ is

$$\frac{\phi^2}{\Lambda^2} = \begin{cases} 3 \left(1 - \frac{\pi}{4\alpha_3} \right) & \frac{\pi}{4} \leq \alpha_3 \leq \frac{3\pi}{8} \\ \frac{2\alpha_3}{\pi} \left(1 + \sqrt{1 - \frac{\pi}{3\alpha_3}} \right) & \alpha_3 > \frac{3\pi}{8} \end{cases}. \quad (3.3.20)$$

The general form of Eqs. (3.3.15)–(3.3.20) are obtained by the replacement

$$\sigma^2 \rightarrow \sigma^2 + \vec{\pi}^2, \quad (3.3.21)$$

$$\phi^2 \rightarrow \bar{\phi}_{\mu c} \phi^{\mu c} + \vec{\delta}_{\mu c} \cdot \vec{\delta}^{\mu c}, \quad (3.3.22)$$

following the symmetry properties of V_{eff} . The transition is of second order across boundaries between 0-phase and the α -phase ($\alpha_0 = \pi/12$) as well as 0-phase and β -phase ($\alpha_3 = \pi/4$) in Fig.3.2; it is first order phase transition across the boundary between α - and β - phase ($\alpha_0 \geq \pi/12$ and $\alpha_3 \geq \pi/4$).

The chiral $SU(2)_L \times SU(2)_R$ symmetry is spontaneously broken down to a $SU(2)_V$ flavor symmetry both in the α -phase and in the β -phase.

Some of the other properties of the β -phase are discussed in more detail in Refs. [5]. They are not reproduced here.

3.4 Spontaneous separation of baryon number in the β - and ω - phases

The vacuum of the models introduced are studied based on the assumption that the lowest energy state of the system (vacuum) contains vanishing baryon number density. This assumption can be phrased in a different way, namely, that the baryon number and the antibaryon number in the vacuum of the system cancel locally leading to net baryon number density zero at each space-time point. This assumption is not apparent a priori since it is not an independent one. Whether or not it is true depends, as it is shown in this study, upon the interaction of the system. Can the vacuum state of an interacting system contains net baryon density locally? The answer is yes [4, 6].

To investigate this question, a Lagrangian density $\tilde{\mathcal{L}}$ differ from the original one Eq. 3.1.1 by an additional $\mu_\alpha j_B^\alpha$ term, with μ^α a statistical gauge field [6] and j_B^α the baryon number current density, can be used [4]. In the 8-component representation for the Dirac spinor, it takes the following form

$$\tilde{\mathcal{L}} = \frac{1}{2} \bar{\Psi} (i \not{\partial} + O_3 \not{\mu}) \Psi + \mathcal{L}_{int}. \quad (3.4.23)$$

In the equilibrium statistical mechanics formulated in a path integration Language, such an additional term is the one needed in a grand-canonical assemble. For the β - and ω - phases, the question of what's the configuration for μ^α in the lowest energy state of the system, which is the one corresponding to the vacuum by definition, can be studied using this Lagrangian density in the conventional formalism treated in the Euclidean space ¹. The resulting effective potential for the ω -phase as a function of $\mu \equiv \sqrt{\mu^2}/\Lambda$ with a definite $\alpha_{3'}$ (and therefore χ^2) is shown in Fig. 3.3. It can be seen that the values for μ that minimize the effective potential are nonzero; this is somewhat counterintuitive. For the β -phase, the result is similar [4]. It is shown in Ref. [6] that in the α -phase, the lowest energy configuration for μ is located at $\mu = 0$.

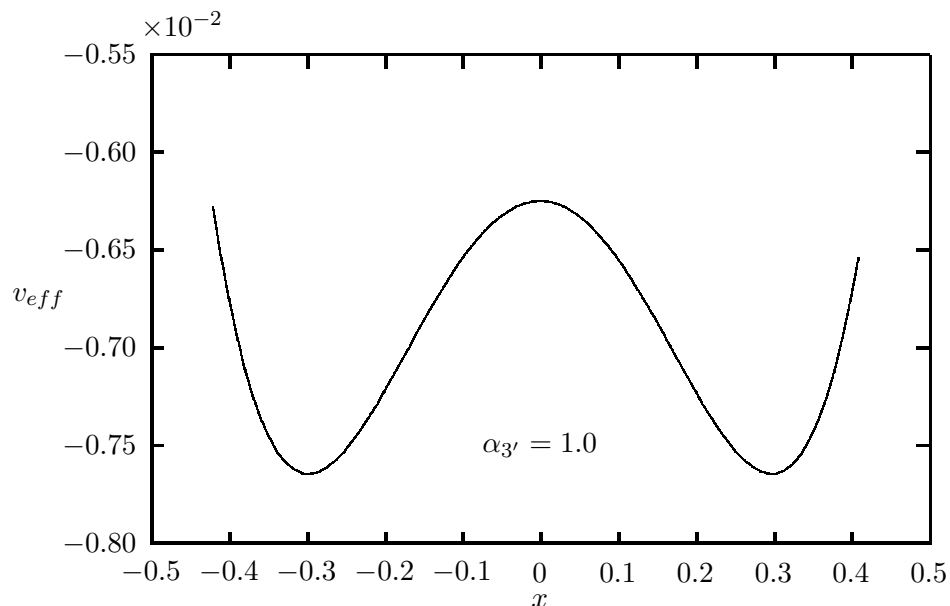


Figure 3.3: The effective potential $v_{eff} = V_{eff}/\Lambda^4$ as a function of $x = \mu/\Lambda$.

A nonvanishing μ implies non-vanishing local baryon number density in the vacuum of the system. It means that *baryon rich and antibaryon rich regions can be generated spontaneously in the β - and ω - phases of the systems considered.* A nonvanishing μ also spontaneously breaks the CP invariance of the original system. These properties of the ω - and β - phases, in which the $U(1)$ phase symmetry corresponding to the baryon number conservation is spontaneously broken down, have the potential of solving [4] the old problem [23] in the idea of the matter–antimatter symmetric universe [24] based on standard big–bang cosmology.

The above mentioned results are actually not difficulty to perceive. In the α -phase, correlated quark–antiquark pairs condense in the vacuum, they can not be spontaneously separated. In the β - and ω -phases, correlated quark–quark pairs and antiquark–antiquark pairs condense; it is conceivable that they prefer to separate locally while keeping the global net baryon number unchanged. This qualitative picture can actually be more rigorously substantiated by using field theoretical method. The details are given in Ref. [6].

¹For a consistent discussion of the α -, β - and ω - phases, certain new computation method has to be introduced. They are given in Ref. [6].

Part II

Traces of β - and ω - Phases in Nuclear Systems

Four possible phases of the light quark system are discovered in Part I of this report. Since the models introduced are not derived from the QCD Lagrangian density, their relevancy can be established either by deducing them from the fundamental theory (QCD) or by checking whether or not the consequences of these models are observable in nuclear systems, like, the static case of inside a nucleon, the dynamical processes involving hadronic reactions, etc.

Deducing the quark-quark interaction terms are not the goal of this research; it is certainly an nontrivial and interesting topic to be studied in the future. The relevancy of the results of the first part of the report are assessed by looking for the possible existence of the phases found there in realistic nuclear systems. Two kinds of systems are considered: 1) inside a nucleon and 2) in the high energy e^+e^- annihilation processes.

The large scale vacuum phase for the strong interaction vacuum is in the α -phase. There are large body of empirical evidences supporting such a notion. The reason behind the search for the β - or ω -phases inside a nucleon and in the hadronization processes of the e^+e^- reaction is inspired by the facts that sufficient high baryon density can cause the strong interaction vacuum to flip into β - or ω - phase [4, 6]. There might be sufficiently high baryon density inside a nucleon and in the hadronization process of the e^+e^- reaction.

The results derived in part I are for a uniform system with its spatial and temporal extension going to infinity. When these results are used in case of a nucleon which is of finite extension in space or in case of an e^+e^- annihilation reaction which is finite both in time duration and spatial extension, fluctuations effects has to be taken into account. Since what is seeking in this work is the null effects, which means that the effects are absent without the existence of the β - or ω - phase, we belief that the question of existence of these phases are not affected by the effects of the fluctuations and a mean field picture is still a good starting point for systematical improvement of the result for technical reasons. This will be elaborated in more detail in the following discussions, which do not depend on mean field pictures.

Chapter 4

Extended PCAC Relation for a Nucleon

4.1 A QCD chiral Ward identity and PCAC relation

The QCD Lagrangian density

$$\mathcal{L} = -\frac{1}{8}\text{Tr}G^{\mu\nu}G_{\mu\nu} + \bar{\psi}(i\not{D} - m_0)\psi, \quad (4.1.1)$$

with $G^{\mu\nu}$ the gluon field strength tensor, ψ the quark field, has a global chiral $SU(2)_L \times SU(2)_R$ symmetry if m_0 is set to zero. There is a QCD Ward identity for the divergence of A_μ^a

$$\partial^\mu A_\mu^a = 2m_0\bar{\psi}i\gamma^5\tau^a\psi \quad (4.1.2)$$

in the $m_0 \neq 0$ case at the “classical” level. Here τ^a (a=1,2,3) is one of the Pauli matrices in the isospin space. Unlike its $U(1)_L \times U(1)_R$ chiral symmetry, which is anomalous, the $SU(2)_L \times SU(2)_R$ chiral symmetry of QCD is anomalies free. Therefore Eq. 4.1.2 continues to be valid when the system gets quantized, which turns it into an operator equation. It has, however, no predictive power in this form since the matrix elements of the right hand side (r.h.s.) of it between physical hadronic states is not immediately known.

The PCAC relation states that

$$\partial^\mu A_\mu^a = m_\pi^2 f_\pi \phi_\pi^a, \quad (4.1.3)$$

While QCD chiral Ward identity follows directly from the QCD Lagrangian, the PCAC relationship is an empirically law, which agrees with data well when $q^2 \sim m_\pi^2 \sim 0$. It implies the following weak equality

$$\phi_\pi^a \sim \bar{\psi}i\gamma^5\tau^a\psi \quad (4.1.4)$$

for their matrix elements in the momentum transfer regions considered.

How does one go from the QCD chiral Ward idnetity Eq. 4.1.2 to the PCAC relation Eq. 4.1.3? How good is it when q^2 is allowed to go away from the pion mass shell? Or, how much difference does one expect between $\partial^\mu A_\mu^a$ and $f_\pi m_\pi^2 \phi_\pi^a$ when their matrix elements between single nucleon states are taken? These questions are studied in this work.

An necessary condition for it to be satisfied is to has its matrix elements between physical hadronic states satisfy the same equation. The PCAC relation in the mesonic sector, namely its matrix elements between meson states, is known to be satisfied. Is it satisfied in the baryonic sector? A closer look at it is necessary in order to have an answer to it.

4.2 PCAC relation for nucleon states

The matrix elements of $\partial^\mu A_\mu^a - f_\pi m_\pi^2 \phi_\pi$ between single nucleon states are parameterized as

$$\langle p' | \partial^\mu A_\mu^a(0) - f_\pi m_\pi^2 \phi_\pi(0) | p \rangle = m_\pi^2 C(q^2) \bar{U}(p') i\gamma^5 \tau^a U(p) \quad (4.2.5)$$

with $C(q^2)$ a measure of the error of the PCAC relationship. In terms of various nucleon invariant form factors, it can be written as

$$q^2 \left[mg_A + (q^2 - m_\pi^2) g_P / 2 \right] + m_\pi^2 [g_{\pi NN} f_\pi - mg_A] = m_\pi^2 (q^2 - m_\pi^2) C(q^2). \quad (4.2.6)$$

Here m is the mass of a nucleon. g_A , $g_{\pi NN}$, f_π and g_P are nucleon axial vector current form factor, the pion-nucleon coupling constant, pion decay constant and the nucleon pseudoscalar form factor respectively. They are functions of both q^2 and m_π^2 .

Let's define two functions

$$A(q^2, m_\pi^2) = 2mg_A + (q^2 - m_\pi^2) g_P \quad (4.2.7)$$

$$B(q^2, m_\pi^2) = g_{\pi NN} f_\pi - mg_A, \quad (4.2.8)$$

where the m_π^2 dependence is written explicitly. It follows from Eq. 4.2.6 that

$$A(q^2, m_\pi^2) = 2m_\pi^2 C(q^2, m_\pi^2), \quad (4.2.9)$$

$$B(q^2, m_\pi^2) = -m_\pi^2 C(q^2, m_\pi^2), \quad (4.2.10)$$

by noting that $A(q^2, m_\pi^2)$, $B(q^2, m_\pi^2)$ and $C(q^2, m_\pi^2)$ are slow varying functions of q^2 so that the coefficient of the explicit q^2 dependent term in Eq. 4.2.6 should vanish (for a more detailed analysis of this assumption, see Ref. [7]).

4.3 Chiral symmetry and two basics relations between nucleon form factors

It can be noted that in the chiral symmetry limit $m_\pi^2 \rightarrow 0$

$$A(q^2, 0) = \lim_{m_\pi^2 \rightarrow 0} [2mg_A + (q^2 - m_\pi^2) g_P] = 0, \quad (4.3.11)$$

which represents the conservation of the axial vector current in that limit. It is also expected that

$$\lim_{q^2 \rightarrow \infty} A(q^2, m_\pi^2) = 0, \quad (4.3.12)$$

which means that the effects of m_0 in the QCD Lagrangian can be neglected when the momentum transfer $q^2 \gg m_\pi^2$. In the region $q^2 \sim m_\pi^2$, $A(q^2, m_\pi^2) = m_\pi^2 C(q^2, m_\pi^2)$, which is small as it will be shown in the following. So, our first basic assumption is

$$A(q^2, m_\pi^2) \approx A(q^2, 0) = 0, \quad (4.3.13)$$

which leads, in the realistic case of $m_0 \neq 0$, to the the following equation

$$mg_A(q^2) + \frac{1}{2}(q^2 - m_\pi^2)g_P(q^2) = m_\pi^2 C(q^2, m_\pi^2) \approx 0. \quad (4.3.14)$$

The correction to it is of order $O(m_\pi^2/M_A^2) \sim 1\%$ (M_A is the lightest meson next to pion in the pionic channel). This equation is supported by recent experimental measurements [14, 15] within $0 < -q^2 < 0.2 \text{ GeV}^2$. The agreement of the above relationship with experiments is quite good. It is important further investigation of the relationship between $g_A(q^2)$ and $g_P(q^2)$ can be carried out.

Here, we shall assume Eq. 4.3.14 to be true (within an error of order $m_\pi^2/M^2 \sim m_0/M \sim 1 - 2\%$). Then

$$g_{\pi NN}(q^2)f_\pi(q^2) - mg_A(q^2) = -m_\pi^2 C(q^2, m_\pi^2) \approx 0. \quad (4.3.15)$$

The correction to it is also of order 1%. It is indeed the case on the pion mass shell $q^2 = m_\pi^2$ where the value of $g_A(m_\pi^2)$, $g_{\pi NN}(m_\pi^2)$ and $f_\pi(m_\pi^2)$ can be deduced from experimental data. Data suggests that $m_\pi^2 C(m_\pi^2, m_\pi^2) \sim 1 - 2\%$.

4.4 The determination of valid q^2 region

Let's evaluate the q^2 dependence of $C(q^2, m_\pi^2)$ so that the range of validity of Eqs. 4.3.14 and 4.3.15 can be assessed by using an once subtracted sum rule, namely

$$C(q^2) = C(m_\pi^2) + \frac{q^2 - m_\pi^2}{\pi} \int_{s_{th}}^{\infty} \frac{ImC(s)}{(s - q^2)(s - m_\pi^2)}, \quad (4.4.16)$$

where the m_π^2 dependence of $C(q^2, m_\pi^2)$ is suppressed for simplicity. Since at small $|q^2|$, the details of $ImC(s)$ is not important, we can use a step function to make an estimate, namely, $ImC(s) \approx \alpha\theta(s - s_{th})$, with $m_\pi^2\alpha \sim 1 - 2\%$. In this simplified case

$$C(q^2) = C(m_\pi^2) + \frac{\alpha}{\pi} \ln \left(\frac{s_{th} - q^2}{s_{th} - m_\pi^2} \right), \quad (4.4.17)$$

where the m_π^2 dependence of $C(q^2, m_\pi^2)$ is suppressed for simplicity. Since at small $|q^2|$, the details of $ImC(s)$ is not important, we can use a step function to make an estimate, namely, $ImC(s) \approx \alpha\theta(s - s_{th})$, with $m_\pi^2\alpha \sim 1 - 2\%$. In this simplified case

$$C(q^2) = C(m_\pi^2) + \frac{\alpha}{\pi} \ln \left(\frac{s_{th} - q^2}{s_{th} - m_\pi^2} \right). \quad (4.4.18)$$

In order for the corrections to our two basic equations Eqs. 4.3.14 and 4.3.15 to increase by another 1%, $|C(q^2) - C(m_\pi^2)|$ has to increase by 100%, which means that the region of validity of Eqs. 4.3.14

and 4.3.15 is $q^2 < 0.7s_{th}$. The range of validity of these two equations in the negative q^2 region is much smaller than $-0.7s_{th}$.

The next step is to estimate the value of s_{th} . The lowest value of s_{th} in the pionic channel is below $9m_\pi^2$, which corresponds to an anomalous threshold for the three pion state. However, the effective s_{th} correspond to that of the $\rho\pi$ threshold, which is considerably larger than $9m_\pi^2$. This is a consequence of the fact that the underlying dynamics of QCD is chiral invariant except for a small mass term. From this fact the dynamical (operator) equation or QCD chiral Ward identity follows. This dynamical equation ensures that the operator $\bar{\Psi}i\gamma^5\tau^a O_3\Psi$ can only excite a longitudinal vector excitation since it is proportional to the divergence of an axial vector operator field. Therefore the state in which the three pions are all in a s-state is dynamically forbidden. The allowed state which dominates the dispersion relation is the one where two of the three pions have a relative angular momentum of 1, which is itself dominated by the ρ excitation strength. Therefore $s_{th} \sim (m_\rho + m_\pi)^2$ and the range of q^2 in which Eqs. 4.3.14 and 4.3.15 are valid is 30 to 35 times larger than $m_\pi^2 \approx 0.02GeV^2$.

4.5 Test of PCAC relation for a nucleon

Eq. 4.3.15 gives a specific relation between $g_A(q^2)$ and $g_{\pi NN}(q^2)f_\pi(q^2)$. We study whether or not it is consistent with the phenomenology next.

The q^2 dependence of $g_A(q^2)$ in the space-like q^2 region is of a dipole form [16], namely,

$$g_A(q^2) = \frac{g_A(0)}{[1 - q^2/M_A^2]^2}, \quad (4.5.19)$$

with $M_A \approx 1$ GeV. We shall use $M_A = 1.0$ GeV in the following.

The q^2 dependence of $g_{\pi NN}(q^2)$ is known less well than that of $g_A(q^2)$. A monopole form for it, which can be parameterized as

$$g_{\pi NN}(q^2) = g_{\pi NN} \frac{\Lambda_{\pi NN}^2 - m_\pi^2}{\Lambda_{\pi NN}^2 - q^2} \quad (4.5.20)$$

is agreed upon in the literature; the value for $\Lambda_{\pi NN}$ varies. It is found to be greater than 1.2 GeV in nucleon-nucleon (NN) scattering and deuteron property studies. It is in contradiction to the expectations of many chiral nucleon models for the nucleon. Lattice QCD evaluation also indicates a smaller one, namely, $\Lambda_{\pi NN} \sim 800$ MeV. On the phenomenological side, Goldberger-Treiman discrepancy study [17], $pp\pi^0$ v.s. $pn\pi^+$ coupling constant difference [18], high energy pp scattering [19] and charge exchange reaction [20, 22], etc, support a value of $\Lambda_{\pi NN}$ close to 800 MeV. By introducing a second ‘‘pion’’ π' with mass 1.3 GeV, $\Lambda_{\pi NN}$ can be chosen to be around 800 MeV without spoiling the fit to the NN scattering phase shifts and deuteron properties [21]. This picture was later justified by a microscopic computation in Ref. [22].

The q^2 dependence of $f_\pi(q^2)$ is little known from direct experimental observations. It can be extracted from the following time ordered correlator

$$q_\mu f_\pi(q^2)\delta^{ab} = -\frac{1}{Z_\pi}(q^2 - m_\pi^2) \int d^4x e^{iq \cdot x} \langle 0 | T \phi_\pi^a(x) A_\mu^b(0) | 0 \rangle_{(-)}. \quad (4.5.21)$$

The pion is a composite particle in QCD. Eq. 4.5.21 can nevertheless be constructed using the following procedure. First, consider a three point function with two quark fields (in the pionic channel)

and one axial vector current operator. It contains a pion pole at $q^2 = m_\pi^2$. Second, solve, e.g., Bethe-Salpeter or whatever suitable equation(s) to obtain the q^2 independent vertex function (or the wave function) for a pion. Third, project out the pion contribution to the three point function at arbitrary q^2 by using certain orthogonality relation¹ between the pion vertex functions and the other parts of the quark-antiquark scattering amplitude (the four point function) in the pionic channel. Therefore the correlator in the above equation can in principle be computed from the QCD Lagrangian. The result is also expected to be unique. It is however hard in practice to obtain a reasonable result since QCD has not been solved. We need to resort to more controllable methods that connect to experimental data and is accurate enough.

At low q^2 , it is beneficial to express it in terms of an once subtracted dispersion relation, namely,

$$f_\pi(q^2) = f_\pi(m_\pi^2) + \frac{q^2 - m_\pi^2}{\pi} \int_{s_{th}}^{\infty} ds' \frac{Imf_\pi(s')}{(s' - q^2)(s' - m_\pi^2)}. \quad (4.5.22)$$

This is because the resulting $f(q^2)$ does not depend on detailed shape of $Imf_\pi(q^2)$ but only some low moments of it when q^2 is sufficiently small. The lightest physical state connects to the axial vector current operator with the quantum number of pion is the $\rho\pi$ two particle state, the value of s_{th} is chosen to be $(m_\rho + m_\pi)^2$, where $m_\rho = 770$ MeV. At $s' = 4m_N^2$, which correspond to the lowest invariant mass of a $\bar{N}N$ system, another branch cut for $f_\pi(q^2)$ develops. We shall include $\rho\pi$ state only since $\bar{N}N$ state contributions to the above equation is small when q^2 is small. Our next step involves the specification or computation of $Imf_\pi(s)$ by exploring the fact that only the $\rho\pi$ state which couples to the pion contributes to $Imf_\pi(s)$ in the momentum transfer region of interest to this paper. An one loop computation of $Imf_\pi(s)$ is known to be insufficient to account for experimental data in other studies [21, 22], the $\rho\pi$ correlation, which forms a resonance near 1.3 GeV, is required. We therefore propose the following form for $Imf_\pi(s)$,

$$Imf_\pi(q^2) = \frac{3}{4} \frac{m_N}{g_{\pi NN}} \frac{g_{\rho\pi\pi}^2}{4\pi} \bar{\rho}_{\pi,\rho\pi}(q^2) \quad (4.5.23)$$

with the reduced density of state

$$\bar{\rho}_{\pi,\rho\pi}(q^2) = \bar{\rho}_0(q^2) \left(1 + \frac{\lambda I_B}{(q^2 - s_B)^2 + \bar{\rho}_0^2(q^2) I_B^2} \right) \quad (4.5.24)$$

and

$$\begin{aligned} \bar{\rho}_0(q^2) = & \sqrt{1 - \frac{(m_\rho + m_\pi)^2}{q^2}} \sqrt{1 - \frac{(m_\rho - m_\pi)^2}{q^2}} \left(1 - \frac{m_\rho^2 - m_\pi^2}{3q^2} \right) \\ & \theta[q^2 - (m_\rho + m_\pi)^2], \end{aligned} \quad (4.5.25)$$

where $\theta(x)$ is the step function with a value of unity for positive x , s_R is chosen to be 1.69 GeV², λ characterizes the strength of the $\rho\pi$ resonance in $Imf_\pi(q^2)$ and $\bar{\rho}_0(s_R)I_B$ characterizes the width of the resonance.

The above form is chosen so that when $\lambda = 0$, $Imf_\pi(q^2)$ is the one loop result in the Feynman-t' Hooft gauge (for the ρ propagator). The $\rho\pi\pi$ interaction piece of Lagrangian density used for evaluation of $Imf_\pi(q^2)$ is

$$\mathcal{L}_{\rho\pi\pi} = g_{\rho\pi\pi} \epsilon^{abc} \pi^a \partial^\mu \pi^b \rho_\mu^c. \quad (4.5.26)$$

¹The orthogonality relation between vertex functions in the relativistic case may need generalization. It is however expected to exist and to be unique. So the projection procedure is not ambiguous. In many analytic diagrammatical calculations based on simple models, the pion contribution term can simply be read out from the three point function.

The corresponding piece of the axial vector current operator, which can be obtained from the Noether theorem, can be written as

$$A_\mu^a = g_{\rho\pi\pi} \frac{m_N}{g_{\pi NN}} \epsilon^{abc} \pi^b \rho_\mu^c, \quad (4.5.27)$$

where use has been made of the linear σ model relation $m_N = g_{\pi NN} \sigma$.

The value for λ , $\Lambda_{\pi NN}$ and I_B is adjusted so that the minimum value of the following function

$$f(\lambda, \Lambda_{\pi NN}, I_B) = \frac{1}{N} \sum_{k=0}^N \frac{[m_N g_A(q_k^2) - g_{\pi NN}(q_k^2) f_\pi(q_k^2)]^2}{m_N^2 g_A^2(q_k^2)} e^{3q_k^2}, \quad (4.5.28)$$

with $q_k^2 = q_{min}^2 + k(q_{max}^2 - q_{min}^2)/N$, is achieved. The value of N is chosen to be 100. $q_{min}^2 = -0.6$ GeV² and $q_{max}^2 = 0.2$ GeV². The factor e^{3q^2} is used to put more weight on small $|q^2|$ region where the fit tends to be poor.

In all cases studied and presented in table 4.1, $\Lambda_{\pi NN} < 0.95$ GeV. If a value $g_{\rho\pi\pi}^2/4\pi = 1.0$ is taken,

Table 4.1: The results of fitting, where $g_A = 1.26$, $g_{\pi NN} = 13.4$, $f_\pi = 93.2$ MeV, $q_{min}^2 = -0.6$ GeV² and $q_{max}^2 = 0.2$ GeV². The unit for all but λ and $g_{\rho\pi\pi}$ is GeV. λ and $g_{\rho\pi\pi}$ are dimensionless. The quantities with a star on top is chosen by physical considerations.

$g_{\rho\pi\pi}^2/4\pi$	$\Lambda_{\pi NN}$	λ	$\sqrt{I_B}$	$\sqrt{s_R^*}$	M_A^*	$\sqrt{s_{th}^*}$
1.0	0.94	1.12	1.12	1.30	1.00	0.91
1.5	0.93	0.41	1.26	1.30	1.00	0.91
2.0	0.91	-0.0023	1.34	1.30	1.00	0.91
2.5	0.89	-0.25	1.27	1.30	1.00	0.91
2.9	0.88	-0.39	1.30	1.30	1.00	0.91
3.5	0.86	-0.56	1.35	1.30	1.00	0.91

the qualitative shape of $Imf_\pi(q^2)$ in Fig. 4.1 obtained by a minimization of Eq. 4.5.28 is similar to the $Im\Gamma(q^2)$ of Ref. [22]. Quantitatively, it has a broader width. The phenomenological value for $g_{\rho\pi\pi}$ can be deduced from the $\rho \rightarrow \pi\pi$ decay process. It has a value satisfies $g_{\rho\pi\pi}^2/4\pi \approx 2.9$. Using this value of $g_{\rho\pi\pi}$, $Imf_\pi(q^2)$ is obtained by minimization. The result is given in Fig. 4.1. It's drastically different in shape from that of $Im\Gamma(q^2)$ in Ref. [22]. In fact, instead of increasing the density of states relative to the one loop result, the resonance contribution decreases the density of states in order to satisfy Eq. 4.3.15. The reduction of density of state indicates either the solution is unphysical (for a normal resonance) or there is a competing resonance in another channel that couples to the pionic channel we are dealing with. But what can the "other resonance" channel be? There is no known resonance there. There seems to be an inconsistency.

Of course this conclusion has to be checked by other computations of $Imf_\pi(q^2)$ in different model Lagrangians or in more fundamental ones like the lattice QCD calculation. It is a worthy topic to be examined in the future.

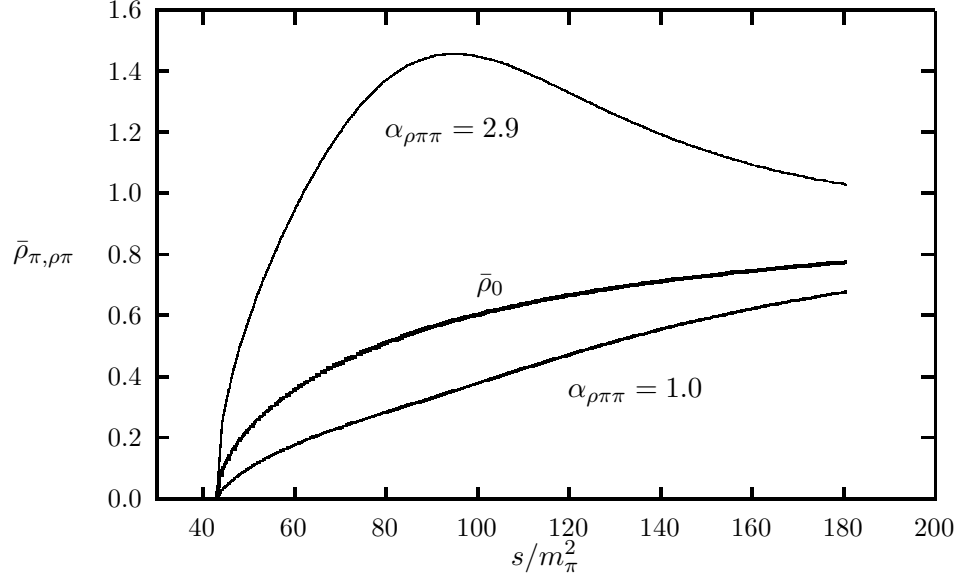


Figure 4.1: The $\rho\pi$ reduced density of states in the pionic channel as a function of q^2 obtained from the fitting procedure for two values of the $\rho\pi\pi$ coupling constant. For comparison, the one loop ($\lambda = 0$) reduced density of state is drawn with a dotted line. Here $\alpha_{\rho\pi\pi} \equiv g_{\rho\pi\pi}^2/4\pi$.

4.6 Extended PCAC relation for a nucleon

Two relationships between experimentally accessible nucleon form factors $g_A(q^2)$, $g_P(q^2)$ and $g_{\pi NN}(q^2)$ and the less well known $f_\pi(q^2)$ off the pion mass shell are established based on the facts that 1) the QCD Lagrangian has an approximate $SU(2)_L \times SU(2)_R$ symmetry, which is explicitly broken down only by a small current mass term (see Eq. 4.1.1) 2) this chiral symmetry is spontaneously broken down to an flavor $SU(2)_V$ symmetry with pion, which is lighter than it should be as an ordinary hadron, as the Goldstone boson of the symmetry breaking 3) the pion, being lighter than other normal hadronic particles, should dominate the low momentum transfer reactions in certain channel, which is expressed as the PCAC relation given by Eq. 4.1.4.

The first relation Eq. 4.3.14 passed the experimental test using the available data. The second one seems to be in trouble when it is confronted with our empirical knowledge. In general, if the deviation is finally established, the remedy for it can be either at a fundamental level, which means to modify the contemporary field theoretical framework or QCD, or at the structural level in the sense of revising our notion of what the structure of the physical system under investigation is. We adopt the second alternative in the following since even if the unlikely possibility that the inconsistency discussed in the above section is finally eliminated after more detailed study, it is still an intellectual challenge how the PCAC relation for a nucleon can be extended within the current theoretical frame work. After all, it is hard to imagine the portion of the vacuum state inside a nucleon remains unchanged under the influence of the baryon density of the valence quarks that are compacted into a region of order 1 fm.

The basic idea of the current approach to extend the PCAC relation consists of a modification of the correspondance Eq. 4.1.4 when its matrix elements are taken between nucleon states by assuming that besides the pion, there is a different set of soft modes inside a nucleon originating from the spontaneous

breaking of the chiral $SU(2)_L \times SU(2)_R$ symmetry down to the same flavor $SU(2)_V$ symmetry. Such a possibility is theoretically investigated in Refs. [4, 5] and are presented in the first part. If there are such a set of these soft modes inside a nucleon, then the left hand side (l.h.s.) of Eq. 4.1.4 in the low momentum transfer regions is saturated not only by the pions, but also these soft modes (Goldstone diquark excitations), which exist if a localized β -phase is assumed.

These color carrying soft modes are confined inside the nucleon and therefore can not be directly observed like the pions but can have an effect by have non-pole contributions to Eq. 4.3.15. The result [7] is

$$mg_A(q^2) = g_{\pi NN}(q^2)f_\pi(q^2) + (q^2 - m_\pi^2)\tilde{\eta}(q^2), \quad (4.6.29)$$

where $\tilde{\eta}(q^2)$ is a function related to the product of the strength of the Goldstone diquark excitations and their propagator, which has no pole at low energies (see Ref. [8] for a more careful discussion on this point) due to the fact that they are confined inside the nucleon. It is worth mentioning that the additional term has no effects on the pion mass shell $q^2 - m_\pi^2$ due to the $q^2 - m_\pi^2$ factor.

With this term added, the potential inconsistency between theory and data discussed in the previous section can in principle be resolved. It is clearly interesting to further investigate the existence or the extend of the inconsistency discussed using various other models and computation procedures.

Chapter 5

Gerasimov–Drell–Hearn Sum Rule for a Nucleon

The Gerasimov–Drell–Hearn (GDH) sum rule [25, 26] is a relation between the difference of two polarized total photon–spin-1/2 Dirac particle cross sections and the corresponding particle’s anomalous magnetic moment. It can be expressed as

$$\int_0^\infty \frac{\sigma_{3/2}(\nu) - \sigma_{1/2}(\nu)}{\nu} d\nu = \frac{2\pi^2 \alpha_{em}}{m^2} \kappa^2, \quad (5.0.1)$$

where $\alpha_{em} = 1/137$ is the fine structure constant, $\sigma_{3/2}$ is the total cross section when the photon helicity is in the same direction as the target particle’s spin polarization, $\sigma_{1/2}$ is the one when the photon helicity antiparallels to the particle’s spin polarization and κ is the anomalous magnetic moment of the particle.

It can be derived if the corresponding forward photon–particle scattering amplitude decreases fast enough at high energies so that an unsubtracted dispersion relation for the amplitude can be written down. For the case of photon–nucleon scattering, the large energy behavior can be inferred from phenomenology, which tells us that the GDH sum rule ought to be satisfied. The current confrontation of the GDH sum rule for a nucleon to known experimental data from pion photo-production result in disagreement [27, 28]. What causes the discrepancy is not yet clear.

Maybe the experimental information used to saturate the l.h.s. of Eq. 5.0.1 is not enough. It may also be that there is a true need of an extension of the GDH sum rule on the theoretical part. This study focus its attention to a theoretical study of the possibility of an extension of the GDH sum rule consistent with Lorentz covariance and local electromagnetic (EM) gauge invariance using the field theoretical methods. We shall review briefly various issues concerning the modification of the GDH sum rule proposed. Details are given in Refs. [8, 39].

5.1 Photon–nucleon compton scattering

The photon–nucleon forward Compton scattering amplitude is related to the following covariant one photon irreducible correlator between EM current operator $J^\mu(x)$

$$T^{\mu\nu}(p, q) = i \int d^4x e^{iq \cdot x} \langle pS | T^* J^\mu(x) J^\nu(0) | pS \rangle, \quad (5.1.2)$$

where $|pS\rangle$ is a nucleon state with 4-momentum p^μ , polarization S^μ and T^* represents time ordering with proper Schwinger terms added. Taking into account of the conservation of parity in the EM interaction, the amplitude can be parameterized by eight invariant amplitudes $F_{1...8}$ the following way

$$T^{\mu\nu}(p, q) = \frac{1}{2m} \bar{U}(pS) [F_1 g^{\mu\nu} - F_2 q^\mu q^\nu + F_3 p^\mu p^\nu - F_4 (p^\mu q^\nu + p^\nu q^\mu) + iF_5 \sigma^{\mu\nu} + iF_6 (p^\mu \sigma^{\nu\alpha} q_\alpha - p^\nu \sigma^{\mu\alpha} q_\alpha) + iF_7 (q^\mu \sigma^{\nu\alpha} q_\alpha - q^\nu \sigma^{\mu\alpha} q_\alpha) + iF_8 \epsilon^{\mu\nu\alpha\beta} q_\alpha p_\beta \not{q} \gamma^5] U(pS). \quad (5.1.3)$$

The invariance amplitudes $F_{1...8}$ are functions of q^2 and $\nu = p \cdot q/m$ with m the mass of a nucleon.

Since the amplitude $T^{\mu\nu}$ satisfies the Ward identity

$$q_\mu T^{\mu\nu}(p, q) = 0 \quad (5.1.4)$$

due to the gauge invariance and commutativity of the EM charge density operators at equal-time, it is usually written in a reduced form, namely,

$$T^{\mu\nu}(p, q) = S_1 \left(-g^{\mu\nu} + \frac{q^\mu q^\nu}{q^2} \right) + S_2 \left(p^\mu - \frac{m\nu}{q^2} q^\mu \right) \left(p^\nu - \frac{m\nu}{q^2} q^\nu \right) - iA_1 \epsilon^{\mu\nu\alpha\beta} q_\alpha S_\beta - im\nu A_2 \epsilon^{\mu\nu\alpha\beta} q_\alpha \left(S_\beta - \frac{S \cdot q}{m\nu} p_\beta \right) \quad (5.1.5)$$

with

$$S_1(q^2, \nu) = -F_1(q^2, \nu) = -q^2 F_2(q^2, \nu) - m\nu F_4(q^2, \nu), \quad (5.1.6)$$

$$S_2(q^2, \nu) = F_3(q^2, \nu) = \frac{q^2}{m\nu} F_4(q^2, \nu), \quad (5.1.7)$$

$$A_1(q^2, \nu) = mF_6(q^2, \nu) + \nu F_8(q^2, \nu), \quad (5.1.8)$$

$$A_2(q^2, \nu) = \frac{1}{m} F_7(q^2, \nu) + F_8(q^2, \nu). \quad (5.1.9)$$

The forward cross section of the compton scattering is related to the amplitude M_{fi} given in to following

$$M_{fi} \sim \epsilon'^*_\mu \epsilon_\nu T^{\mu\nu} \quad (5.1.10)$$

where ϵ' and ϵ are the final and initial photon polarizations. In the nucleon rest frame, the polarization dependent part of the forward cross section depends only on A_1 when the nucleon polarization direction $S^\mu = (0, \vec{S})$ is along direction of the photon propagation.

The invariant amplitude A_1 enjoys a sum rule given by Eq. 5.0.1. Its derivation involves three issues discussed in the following 1) is the use of the infinite momentum frame legitimate? 2) can the high energy (ν) behavior of $A_1(q^2, \nu)$ be estimated using the Regge asymptotics? 3) what's the role of gauge invariance in determining the large ν behavior of $A_1(q^2, \nu)$?

5.2 Sum rules and infinite momentum frame

The need of using an infinite momentum frame in deriving a fixed q^2 sum rule like the GDH sum is discussed and emphasised in Ref. [29]. It's validity in the derivation is generally assumed. It is also assumed in this work.

5.3 Regge behaviors and physical states

The large energy physical hadronic scattering amplitudes follow certain power law (in energy) according to Regge asymptotics [30], namely

$$\lim_{\nu \rightarrow \infty} A \sim \nu^\alpha \quad (5.3.11)$$

where ν is the energy variable and α is the leading Regge trajectory of the corresponding channel. The highest trajectory is that of the Pomeron with an $\alpha(0) = 1$ [31]. Since the Pomeron has a spin one (in the forward direction), it can not be exchanged in some channels of reaction due to helicity conservation; this allows the corresponding amplitude to change slower than ν . If the change is slow enough, it allows certain superconvergence relation to be derived for it in the corresponding channel for physical hadronic scattering amplitude [29].

The problems of using Regge asymptotic behavior in deriving sum rules for matrix elements of a current (between physical hadronic states) is known from current algebra studies [32, 33], in which it was found that a hypothetical case of isovector photon–nucleon scattering there appears the need of a “J=1 fixed pole” in the amplitude for the matrix elements of the time ordered current–current correlator. This problem can be understood if one realizes that the matrix elements of the time ordered current–current correlator does not correspond to a 4–points physical hadronic scattering amplitude directly. The phenomenological Regge asymptotics may fail for these amplitudes. This situation opens the door for a modification of those sum rule that are derived under the assumption of Regge behavior for the matrix elements of the time ordered current–current correlator. For the GDH sum rule, this is suggested in Refs. [34, 35].

For the realistic photon–nucleon scattering, this kind of “J=1 fixed pole” effects can not be straight forwardly introduced in such a way that the results are consistent with current algebra. This is because it causes a modification of the commutation relation between the time component of the EM current operator at equal-time, which tells us that they commute with each other. This requirement, together with gauge invariance, are expressed simply by Eq. 5.1.4. A modification of the commutation relation between the charge density operators at equal-time is suggested in Refs. [36, 37]. It leads to a modification of the Ward identity Eq. 5.1.4, so that a mutual consistency of the arguments can be maintained. Whether or not such a way of modifying GDH sum rule actually is consistent with phenomenology remains to be shown however.

5.4 Gauge invariance constraints

The scheme proposed in this study is different in that the GDH sum rule is modified by introducing an effective “J=1 fixed pole” effect without modifying the commutation relation between the charge density operators at equal-time. This is achieved by assuming there is a localized breaking down of the $U(1)_{em}$ gauge symmetry inside a nucleon [8]. The “J=1 fixed pole” effects are provided by the would-be Goldstone boson of the symmetry breaking, which does not belong to physical excitation spectrum for a local gauge symmetry [38].

From the Ward identity Eq. 5.1.4, there are three constraints for $F_{1\dots 8}$ in Eq. 5.1.3, namely,

$$F_1(q^2, \nu) - q^2 F_2(q^2, \nu) - m\nu F_4(q^2, \nu) = 0, \quad (5.4.12)$$

$$m\nu F_3(q^2, \nu) - q^2 F_4(q^2, \nu) = 0, \quad (5.4.13)$$

$$F_5(q^2, \nu) - m\nu F_6(q^2, \nu) - q^2 F_7(q^2, \nu) = 0. \quad (5.4.14)$$

Eq. 5.4.14 is relevant to the possibility of modifying the GDH sum rule.

The large ν behavior of $F_5(q^2, \nu)$ can be determined to be [8] $F_5 \sim \nu^{-1}$. If the following assumption is made, namely,

$$\lim_{q^2 \rightarrow 0} q^2 F_7 = 0, \quad (5.4.15)$$

then the large ν behavior of F_6 at $q^2 = 0$ is ν^{-2} following Eq. 5.4.14. Under the assumption given by Eq. 5.4.15, the large ν behavior of A_1 , which is relevant to the GDH sum rule, is controlled by that of F_8 . The large ν behavior of F_8 is bounded by the Regge asymptotics because it is an gauge invariant amplitude by itself, which means that it connects to physical scattering amplitude only (for a detailed discussion on this point, see Refs. [8, 39]). Thus $F_8 \sim A_1 \sim \nu^{\alpha-1}$ with $\alpha < 1$ from helicity amplitude analysis [40]. Thus gauge invariance requirement expressed by Eq. 5.1.4 together with Eq. 5.4.15 eliminates the possibility of a modification of the GDH sum rule.

5.5 The possibility of modifying GDH sum rule

The above analysis show that if GDH sum rule is to be modified in a way that respect the local EM gauge invariance and the Regge asymptotic behavior for physical hadronic scattering amplitudes, assumption Eq. 5.4.15 has to be relinquished by letting F_7 to has a pole like behavior¹ in q^2 at large ν . This implies that the $U(1)_{em}$ symmetry corresponding to EM is spontaneously broken down inside a nucleon [8]. More specifically, introducing an order parameter ρ_∞ , defined as

$$\rho_\infty = - \lim_{q^2 \rightarrow 0} \lim_{\nu \rightarrow \infty} \frac{q^2 F_7}{\nu} \quad (5.5.16)$$

for the EM gauge symmetry inside a nucleon². If the $U(1)_{em}$ gauge symmetry is spontaneously broken down, then there is a massless pole in F_7 in the $\nu \rightarrow \infty$ limit so that ρ_∞ can be nonzero. With ρ_∞ , the GDH sum rule is modified to

$$\int_0^\infty \frac{\sigma_{3/2}(\nu) - \sigma_{1/2}(\nu)}{\nu} d\nu = \frac{2\pi^2 \alpha_{em}}{m^2} (\kappa^2 + 2m^2 \rho_\infty). \quad (5.5.17)$$

Numerically, the value for ρ_∞^p and ρ_∞^n and their difference can be extracted from the results of the integration of the total photon–nucleon cross sections given in Ref. [28]. They take the value $\rho_\infty^p = 2.9 \times 10^{-2} fm^2$ and $\rho_\infty^n = -2.5 \times 10^{-2} fm^2$. As a final remark for this section, it should be mentioned that $\rho_\infty^{p,n}$ has a dimension of length squared. It can be written as $\rho_\infty^{p,n} = 1/\Lambda^2$. It is interesting to note that $\Lambda \sim 1 GeV$, which correspond to the natural scale of the spontaneous chiral symmetry breaking in strong interaction.

It shows that if the current discrepancy between cross section $\sigma_{3/2}$ and $\sigma_{1/2}$ obtained from the the photo pion production on a nucleon data and the GDH sum rule is genuine, then a localized spontaneous breaking down of the $U(1)_{em}$ symmetry inside a nucleon has to be introduced. As it is discussed in part I of this report, such a symmetry breaking is in principle possible since the $U(1)_{em}$ gauge symmetry is spontaneously broken down in the β - and ω - phases [5, 4].

¹Ref. [8] provides a more precise meaning for this statement.

²The first limit $\nu \rightarrow \infty$ is necessary since localized spontaneous gauge symmetry breaking is discussed here. A finite region in space only looks more and more like an infinite system when smaller and smaller distances or higher and higher energies are probed.

Chapter 6

Rapidity Correlation of $B\bar{B}$ in High Energy e^+e^- Annihilation

The hadronization processes in the e^+e^- annihilation can be described reasonably well by a chain like picture in terms of string (or flux tube) fragmentation. For the meson production, quark and antiquark pair is created by a breaking of the string that connects the parent quark-antiquark pairs. At the breaking point, any nonvanishing conserved quantum number like charge, baryon number, etc. are created in conjugate pairs so that they cancel locally (in space-time) there. The reason behind it is that the string is considered to be neutral in these quantum numbers. Monte Carlo simulation programs like the JETSET [41] and Herwig [42], which are based upon such a picture describe the experimental data well.

This picture of hadronization implies strong rapidity correlation between pairs of hadrons that conjugate to each other in the multihadron final state. Since, before the string fragmentation, it is in a stage of uniform expansion, the neighboring hadrons produced on the string by a fragmentation has rapidity close to each other than others. It is difficult to test the consequences of this picture using the mesonic component of the final state since 1) the correlating meson pairs are hard to identify and 2) the interaction between the mesonic particles are stronger than that of the baryons in the e^+e^- annihilation. The interaction distorts the rapidity information of the meson at the time when it is created. On the other hand, larger than 50% of the baryons escape the hadronic clouds before interaction effects grow; they therefore carry the rapidity information at their production time [9]. One of the best characters of the string fragmentation picture for hadronization in the e^+e^- annihilation processes is the strong rapidity difference correlation between a pair of baryon and antibaryon ($B\bar{B}$).

The experimental examination of it was carried out by observing the $\Lambda\bar{\Lambda}$ rapidity difference correlation [10] in e^+e^- annihilation at $\sqrt{s} = 91$ GeV by OPAL collaboration. A “surprise” was found that the width of the rapidity difference correlation between $\Lambda\bar{\Lambda}$ pairs are wider than it is expected from the one predicted by the above mentioned fragmentation model, which consists of the creation of diquark-antidiquark pairs on the string for the formation of baryons, similar to the quark-antiquark pair creation for mesons production. In order to describe the data, the so-called popcorn mechanism [43] has to be introduced, and, in addition, the percentage of the popcorn configuration has to be large in the fragmentation processes [9, 10].

The popcorn mechanism implies a non-local production of conjugate baryon number pairs on the string under the fragmentation since, in between them, there has to be a finite space that contains the meson. The conclusion that conjugate baryon numbers carried by diquark and antidiquark on the string

are not created at the same spacetime point is hard to understand if the string that fragments into $B\bar{B}$ pairs are neutral in baryon number. According to the principle of relativity, it violates the classical causality which requires local cancellation of baryon number and antibaryon number at the time when they are created from a baryon neutral source; the speed of their separation should be less than the speed of light.

This difficulty can however be solved if one assumes that there exists β - or ω - phase inside the string under the fragmentation. The reason, as it is discussed in section 3.4 of part I is that, spontaneous separation of baryon numbers are favored in these phases (see, for example, Fig. 3.3). Therefore if one of the above mentioned phases is present inside the string before a fragmentation, the baryon density on the string can be non-zero at a specific point; it is positive or negative alternatively along the string. Thus, by assuming the existence of the β - or ω - phase discussed in part I of the report, we can gain a deeper understanding of the empirical popcorn mechanism needed in phenomenology.

Before closing this short chapter, let's remind the reader that this finding, if proved genuine in the future after more comprehensive studies, could provide a domestic experimental basis¹ for the baryogenesis mechanism in a matter–antimatter symmetric universe [24] under the standard cosmology (big-bang), which is based upon the spontaneous separation of baryonic matter and antibaryonic matter at certain time during the evolution of the univers [4, 6], without violating the observational constraints [23]. It is certainly a worthy topic to be further studied.

¹In the sense that the physical processes underlying the mechanism can be created and studied here, on earth.

Chapter 7

Summary and Outlook

The theoretically possible phases in an interacting massless two flavor quark system are discussed in the chapters of part I of this report by introducing model Lagrangians. Four phases are found. Some of their properties are discussed while others are mentioned with references containing more details provided. In part II, three different observations, which is currently considered difficult to understand using the conventional picture, are discussed in the light of the findings presented in part I of this report. We find it likely that localized diquark condensed phases exist inside a nucleon and hadronic excited states (within the flux tube).

In the heavy ion collisions, baryon number density and the volume containing it can be much larger than that of a nucleon. It is thus very probable that the β - or ω - phase can be produced despite the short time duration of the collision. What signals their existence and how to find them are questions that can be further investigated.

Bibliography

- [1] F. Karsch, E. Laermann, Rep. Prog. Phys. **56** (1993) 1347.
- [2] R. Hagedorn, Nuovo Cim. Suppl. **3** (1965) 147.
- [3] T. Blum, L. Kärkkäinen, D. Toussaint and S. Gottlieb, “The Equation of State for Two Flavor QCD”, contribution to the XIIth International Symposium on Lattice Field Theory (Lattice’94), Bielefeld 1994.
- [4] S. Ying, Phys. Lett. **B283** (1992) 341.
- [5] S. Ying, Ann. Phys. (N.Y.) (1996) in press.
- [6] S. Ying, work in progress.
- [7] Preprint hep-ph-9506290; S. Ying, Comm. Theor. Phys. (1996) in press.
- [8] S. Ying, J. Phys. **G22** (1996) 293.
- [9] Z. G. Si, Q. B. Xie, and Q. Wang, talk given at this workshop.
- [10] OPAL Collab. P. D. Acton, et al., Phys. Lett. **B305** (1993) 415.
- [11] Y. Nambu and G. Jona-Lasinio, Phys. Rev. **122** (1961) 345; Phys. Rev. **124** (1961) 246.
- [12] See, e.g., S. Coleman, R. Jakiw, and H. D. Politzer, Phys. Rev. **D10** (1974), 2491.
- [13] D. Gross and A. Neveu, Phys. Rev. **D10** (1974), 3235.
- [14] S. Choi, et al., Phys. Rev. Lett. **71** (1993) 3927.
- [15] A. S. E Saulov, A. M. Philipenko, and Yu. I. Titov, Nucl. Phys. **B136** (1978) 511.
- [16] A. del Guerra et al., Nucl. Phys. **B107** (1976) 65; W. A. Mann et al., Phys. Rev. Lett. **31** (1973) 844.
- [17] A.S. Coon and M.D. Scadron, Phys. Rev. **C23** (1981) 1150.
- [18] A. Thomas and K. Holinde, Phys. Rev. Lett. **63** (1989) 2025.
- [19] B.A. Li, K.F. Liu, and M.L. Yan, Phys. Lett. **B212** (1988) 108.
- [20] H. Esbensen and T.S. Lee, Phys. Rev. **C32** (1985) 1966; S. Deister, M.F. Gari, W. Kruempelmann, and M. Mahlke, Few-Body Supl. **10** (1990) 1–36.
- [21] K. Holinde and A.W. Thomas, Phys. Rev. **C42** (1990) R1195.

- [22] G. Janssen, J.W. Durso, K. Holinde, B.C. Pearce, and J. Speth, Phys. Rev. Lett. **71** (1993) 1978.
- [23] G. Steigman, Ann. Rev. Astron. Astrophysics **14** 339.
- [24] R. Omnes, Phys. rev. Lett. **23** (1969) 38.
- [25] S. B. Gerasimov, Yad. Fiz. **2** (1965) 598 [Sov. J. Nucl. Phys. **2** (1966)430]; an earlier related work is given in L. I. Lapidus and Chou Kuang-chao JETP **14** (1962) 357.
- [26] S. D. Drell and A. C. Hearn, Phys. Rev. Lett. **16** (1966) 908.
- [27] R. L. Workman and R. A. Arndt, Phys. Rev. **D45** (1992) 1789.
- [28] A. M. Sandorfi, C. S. Whisnant, and M. Khandaker, Phys. Rev. **50** (1994) R6681.
- [29] S. L. Adler and R. F. Dashen, *Current Algebra and Applications to Particle Physics*, (W.A. Benjamin Inc., New York, Amsterdam, 1968).
- [30] See, e.g., Steven C. Frautschi, *Regge Poles and S-matrix Theory*, (W.A. Benjamin Inc., New York, Amsterdam, 1963).
- [31] See, e.g., G. Cocconi et al., Phys. Rev. Lett. **7** (1961) 450; Foloy et al., Phys. Rev. Lett. **10** (1963) 543.
- [32] L. B. Bronzan, I. S. Gerstein, B. W. Lee and F. E. Low Phys. Rev. Lett. **18** (1967) 32.
- [33] V. Singh, Phys. Rev. Lett. **18** (1967) 36.
- [34] H. Abarbanel and M. Goldberger, Phys. Rev. **165** (1968) 1594.
- [35] G. Fox and D. Freedman, Phys. Rev. **182** (1969) 1628.
- [36] K. Kawarabayashi and M. Suzuki, Phys. Rev. **152** (1966) 1383.
- [37] L. N. Chang, Y. Liang, and R. Workman, Phys. Lett. **B329** (1994) 514.
- [38] F. Strocchi, Comm. Math. Phys. **56** (1977) 57.
- [39] Work in progress.
- [40] D. J. Broadhurst, J. F. Gunion and R. L. Jaffe, Phys. Rev. **D8** (1973) 566.
- [41] B. Andersson et al., Phys. Rep. **97** (1983) 31; T. Sjöstrand, Comp. Phys. Commun. **39** (1986) 3473; **43** (1987) 367.
- [42] G. Marchesini et al., Cambridge preprint Cavendish-HEP-91/26; DESY 91-048.
- [43] B. Andersson, G. Gustafson and T. Sjöstrand, Physica Scripta **32** (1985) 574.

